SSRG International Journal of Electrical and Electronics Engineering
ISSN: 2348-8379/ https://doi.org/10.14445/23488379/IJEEE-V11I7P117

Volume 11 Issue 7, 199-207, July 2024

Original Article

Lagrange Theory-Based Optimization Strategy to Minimizing Power Loss of an Electric Power Grid: Theoretical and Experimental Study

Tien-Dung Nguyen[1], Thi-Duyen Bui[1], Ngoc-Khoat Nguyen[1*]

[1]*Faculty of Control and Automation, Electric Power University, Hanoi, Vietnam.*

[*]*Corresponding Author : khoatnn@epu.edu.vn*

Received: 08 May 2024 Revised: 11 June 2024 Accepted: 08 July 2024 Published: 26 July 2024

Abstract - *This study introduces a novel, straightforward, and highly efficient control algorithm aimed at mitigating the reactive power compensation challenge to enhance the power quality of a distribution network. The network under scrutiny is characterized by the presence of high-capacity three-phase induction motors as primary loads. The proposed solution for reactive power compensation employs the NEMA curve to assess power losses across individual motors and throughout the entire network. Subsequently, a Lagrange function is formulated, and Lagrange's theory is applied to ascertain the extremal values of this function, facilitating the computation of the optimal reactive power compensation capacity. The efficacy of the proposed algorithm is theoretically substantiated through simulation results obtained for a typical power system featuring three high-capacity induction motors utilizing the MATLAB software package. Additionally, experimental outcomes acquired from a real-world test case corroborate the substantial efficacy and commercialization potential of this innovative contribution.*

Keywords - *Voltage regulation, Reactive power compensation, NEMA curve, Lagrange theory, Loads of three phase induction motors.*

1. Introduction

The quest for optimal power quality and improved efficiency within electrical infrastructure transcends the boundaries of the power industry itself, impacting a vast array of sectors. This ongoing challenge is well documented in pertinent academic literature [1, 2]. Power quality optimization has risen to paramount importance due to the multifaceted benefits it offers. These advantages encompass not only the fostering of energy efficiency but also the bolstering of competitiveness for businesses that rely on a steady and reliable power supply. Additionally, optimized power quality enhances the safety and reliability of electricity delivery, a critical factor for ensuring the smooth operation of vital services and infrastructure. Furthermore, it extends the lifespan and improves the performance of electrical equipment, ultimately reducing replacement costs and minimizing downtime. Perhaps most significantly, optimized power quality translates to cost savings for electricity consumers across all sectors.

However, the detrimental effects of compromised power quality cannot be overstated. When power quality suffers, the operation of electrical devices can be significantly disrupted. Asynchronous motors, which constitute a substantial portion (45-50%) of the overall electrical load, are particularly vulnerable to these disruptions [3]. Numerous studies have documented the detrimental effects of poor power quality on these motors, including increased power losses, elevated operating temperatures, reduced efficiency, and a shortened lifespan [4, 5]. In simpler terms, a decline in power quality directly translates to a corresponding decline in the efficiency of three-phase asynchronous motor loads. This highlights the critical need for a multi-faceted approach to electrical infrastructure optimization, encompassing not only the generation of clean and reliable power but also efficient transmission and distribution systems that minimize quality degradation.

A variety of voltage regulation techniques exist to enhance voltage quality, including [4, 6]:

- Adjusting Generator Field Current: This method involves altering the excitation current of the generator to regulate voltage output.
- Tap-Changing Transformers: Fixed tap-changing transformers or on-load tap changers can be employed to adjust voltage levels at distribution points.
- Voltage Regulation Transformers and Auxiliary Transformers: These transformers are deployed to compensate for voltage drops along transmission lines.

- Switched Capacitor Banks: Dynamically switching capacitor banks in and out of the system can help maintain voltage stability.
- Load Shedding: During peak demand periods, controlled load shedding can alleviate voltage sags.
- Conductor Size Modification: Increasing conductor size reduces line impedance and voltage drops.
- Harmonic Filtering: These mitigate the detrimental effects of harmonic distortion on voltage quality.
- Reactive Power Compensation: Reactive power compensation techniques, such as Static VAr Compensators (SVCs) and Dynamic VAr Compensators (DVACs), address reactive power imbalances and improve voltage stability.

Several reactive power compensation schemes are utilized in contemporary power systems. Common compensating methods include capacitor banks, synchronous condensers, Static VAr Compensators (SVCs), and shunt compensation (illustrated in Figure 1).

Previous studies have investigated reactive power compensation across diverse network configurations. Report [7] discusses compensation methods for medium and low voltage networks. Our previosu study proposes a novel DC-CC (Distributed Compensation-Central Control) strategy for systems primarily driven by large induction motors. Hardware implementations of SVCs using microcontrollers are detailed in [8]. Meanwhile, reference [9] explores the utilization of STATCOMs for reactive power compensation in interconnected power grids.

Optimization techniques have also been deployed for reactive power management. The Nash Bargaining solution is applied in [10] to attain optimal compensation. Reference [11] introduces a decentralized approach for reactive power sharing and frequency restoration in isolated microgrids. A comparative analysis evaluating various compensating devices is presented in [12].

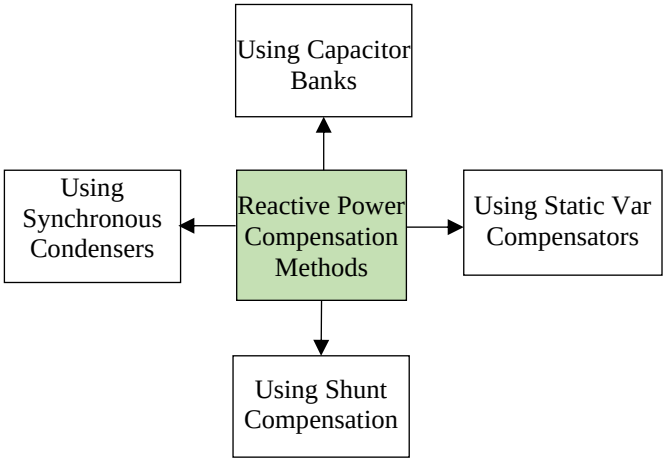

Fig. 1 Reactive power compensation methods

Automatic Voltage Control (AVC) has been deployed for reactive power management in specific regions, as demonstrated by the Wuhu region power grid [13]. Reference [14] outlines a robust control scheme for regulating distribution power networks amidst photovoltaic uncertainty while compensating for reactive power. Lastly, [15] proposes a distributed control scheme specifically tailored for reactive power compensation in smart grids, particularly microgrids.

This work presents a novel and simple reactive power compensation strategy employing a decentralized-centralized control architecture based on Lagrange theory [16]. The primary objective is to regulate grid voltage stability, particularly in power systems where large-capacity induction motors constitute a significant portion of the load. The electrical characteristics of these motors will be accurately modeled using the well-established NEMA standards.

The optimal level of reactive power compensation will be established through the application of the Lagrange multiplier method, a powerful optimization technique. The efficacy of the proposed approach will be rigorously evaluated through a combination of simulated scenarios and real-world experimentation.

The paper is organized as follows. After the introduction, Section 2 presents the application of Lagrange theory to the power loss optimization problem. Then, Section 3 shows the simulation and experiment procedure and results, verifying the applicability of the control strategy proposed in this work. The last section provides significant conclusions regarding this study.

2. Lagrange Theory-Based Optimization Method to Power Loss

The proposed study examines a power distribution layout tailored for a standard industrial plant or factory, as illustrated in Figure 2. This configuration encompasses a high-voltage supply operating at 110kV, high-voltage cabling, a Medium-Voltage Substation (MVS), medium-voltage cables, a Low-Voltage Substation (LVS), three induction motor loads (i = 1÷3), low-voltage cabling, a centralized compensation unit (Q_{bTrt}), and distributed compensation units at each load (Q_{bi1-3}).

All pertinent system parameters are gauged and consolidated within a control cabinet. Subsequently, the system undertakes optimization computations to curtail overall losses and dispenses control directives to the distributed compensation cabinets to furnish the requisite compensation capacitance at each designated site in accordance with the algorithmic directives. Figure 2 delineates the system parameters, encompassing:

- The power (P_i – jQ_i) is produced by the three-induction motor loads.

- The capacities of compensation apparatuses at each load and the centralized compensation unit are identified as Q_{b1}, Q_{b2}, Q_{b3} and Q_{bTrt}, respectively.
- The low-voltage substation at 22kV/0.4kV.
- The transmission line connects the medium-voltage and low-voltage transformers.
- The medium-voltage substation is at 110kV/22kV.
- The lengths of cables extending from the busbar to each of the three motor loads.

Given that the compensation apparatuses are positioned at the terminal juncture of the transmission line, the system parameters are computed relative to the low-voltage facet of the MVS-T2. The power losses incurred due to the operation of the induction motor loads on the power grid in the presence of compensation devices are delineated as:

$$\Delta P = R_{td}\frac{P_{tt}^2+(Q_{tt}-Q_b)^2}{U_{ht}^2} * 10^{-3} + \Delta P_b Q_b + P_{tt}[1 - \eta_{max} - \Delta\eta\{Q_{tt} - Q_b\}] \quad (1)$$

In (1), the following parameters are employed: R_{td}, which is the equivalent resistance of the entire system; P_{tt} and Q_{tt} denote the active and reactive power demands; ΔP_b signifies the active power loss of the compensator.

Additionally, Q_b represents the reactive power compensation while η_{max} is the maximum efficiency of the load and $\eta\{Q_{tt}$-$Q_b)$ denotes the change of efficiency in percentage, calculated by the NEMA curve. The following step-by-step calculations are implemented by applying the NEMA curve, as reported in our previous study.

$$\Delta\eta\{Q_{tt} - Q_b\} = (K_1\Delta U_{DC}^2 + K_2\Delta U_{DC} + C) * 10^{-2} \quad (2)$$

$$\Delta U_{DC} = \frac{U_{DC}-U_{dm\_DC}}{U_{dm\_DC}} * 100 \quad (3)$$

$$U_{DC} = \frac{U_{22}}{U_{11}}U_{ht} * 10^3 - \Delta U \quad (4)$$

$$\Delta U = \frac{P_{tt}R_{td}+(Q_{tt}-Q_b)X_{td}}{U_{ht}} \quad (5)$$

$$\Delta P = R_{td}\frac{P_{tt}^2+(Q_{tt}-Q_b)^2}{U_{ht}^2} * 10^{-3} + \Delta P_b Q_b + P_{tt}[-\Delta\eta\{Q_{tt} - Q_b\}] \quad (6)$$

$$\Delta P_{\Sigma} = \sum_{i=1\div3}\left[R_{l_i}\frac{P_i^2+(Q_i-Q_{bi})^2}{U_{TC}^2} * 10^{-3} + \Delta P_b Q_{bi} + P_i(-\Delta\eta_i\{Q_i - Q_{bi}\})\right] + R_{ht\_tc}\frac{P_{\Sigma}^2+(Q_{\Sigma}-Q_{b\Sigma}-Q_{bTrt})^2}{U_{ht1}^2} * 10^{-3} + \Delta p_{bTrt}.Q_{bTrt} \quad (7)$$

$$Q_{b\Sigma} + Q_{bTrt} = 40\%S_{MBA2} \Longrightarrow Q_{b\Sigma} + Q_{bTrt} - 40\%S_{MBA2} = 0 \quad (8)$$

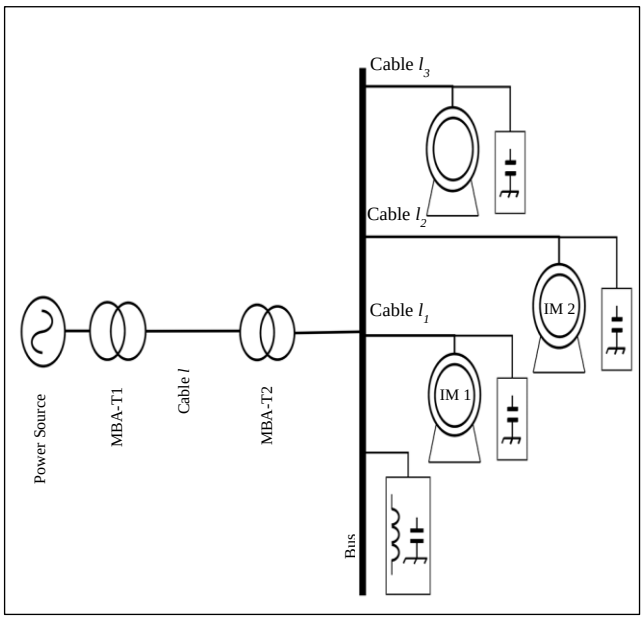

(a)

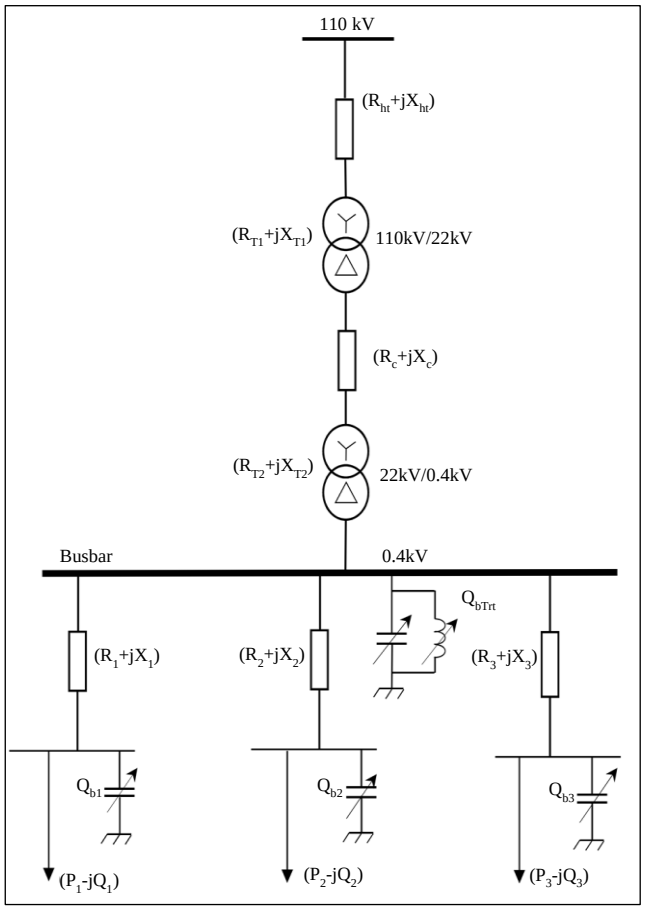

(b)

Fig. 2 Power system model under study (a) and (b)

The details for each parameter and relevant nomenclature can be found in the Appendix of this paper.

The following steps are conducted to apply the Lagrange theory to find the extreme values of the loss total.

- Step 1: Define the Lagrange function as indicated in (9) below.

$$\begin{aligned} L\ (Q_{bi}, Q_{bTrt}, \lambda)\ = & \sum_{i=1\div 3}\left[R_{l_i}\frac{P_i^2+(Q_i-Q_{bi})^2}{U_{TC}^2}.10^{-3}\right. \\ & \left.+\Delta p_b.Q_{bi}+P_i.\left(-\Delta\eta_i\left\{Q_i-Q_{bi}\right\}\right)\right] \\ & +R_{ht\_tc}\frac{P_\Sigma^2+(Q_\Sigma-Q_{b\Sigma}-Q_{bTrt})^2}{U_{ht1}^2}.10^{-3} \\ & +\Delta p_{bTrt}.Q_{bTrt}+\lambda.(Q_{b\Sigma}+Q_{bTrt}-\ 0.4S_{MBA2}) \end{aligned} \tag{9}$$

- Step 2: Calculate the partial derivatives of the Lagrange function as follows:

$$\begin{cases} \dfrac{\partial L\ (Q_{bi}, Q_{bTrt}, \lambda)}{\partial Q_{bi}} = -\dfrac{2.10^{-3}R_{l_i}}{U_{TC}^2}(Q_i-Q_{bi}) \\ +\Delta p_b - P_i.\dfrac{\partial\Delta\eta_i\left\{Q_i-Q_{bi}\right\}}{\partial Q_{bi}} - \dfrac{2.10^{-3}R_{td}}{U_{ht1}^2}(Q_\Sigma-Q_{b\Sigma}-Q_{bTrt})+\lambda \\ \dfrac{\partial L\ (Q_{bi}, Q_{bTrt}, \lambda)}{\partial Q_{bTrt}} = -\dfrac{2.10^{-3}R_{td}}{U_{ht1}^2}(Q_\Sigma-Q_{b\Sigma}-Q_{bTrt})+\Delta p_{bTrt}+\lambda \\ \dfrac{\partial L\ (Q_{bi}, Q_{bTrt}, \lambda)}{\partial \lambda} = Q_{b\Sigma}+Q_{bTrt}-\ 0.4S_{MBA2} \end{cases} \tag{10}$$

- Step 3: Solve the system of equations

$$\frac{\partial L}{\partial x_i} = 0;\ x_i \in \{Q_{bi}, Q_{bTrT}, \lambda\}$$

The solutions are presented below:

$$\begin{cases} Q_{bi} = Q_i - \dfrac{A_{i2}.(\Delta p_{bi}\ -\ \Delta p_{bTrt})\ -\ A_{i3}}{A_{i1}} \\ Q_\Sigma\ -\ Q_{b\Sigma}\ -\ Q_{bTrt}\ = (Q_\Sigma\ -\ 0{,}4S_{MBA2}) \end{cases} \tag{11}$$

Where:

$$\begin{aligned} A_{i1} &= 2R_i.10^{-3}.U_{dm}^2\ -\ 2.10^2.K_1.P_i.X_{li}^{\ 2}; \\ A_{i2} &= \left(U_{dm}.U_{TC}\right)^2; \\ A_{i3} &= P_i.X_{li}.\left\{\begin{matrix} 2.10^2.K_1.\left[\left(U_{TC}.10^3\ -\ U_{dm}\right)U_{TC}\ -\ P_i.R_{li}\right] \\ +K_2.U_{dm}.U_{TC} \end{matrix}\right\} \end{aligned} \tag{12}$$

By implementing the steps mentioned above, a decentralized compensation system integrated with a centralized controller can be effectively established. This control strategy facilitates the solution of the power loss minimization problem, thereby enhancing the performance of an electric power grid.

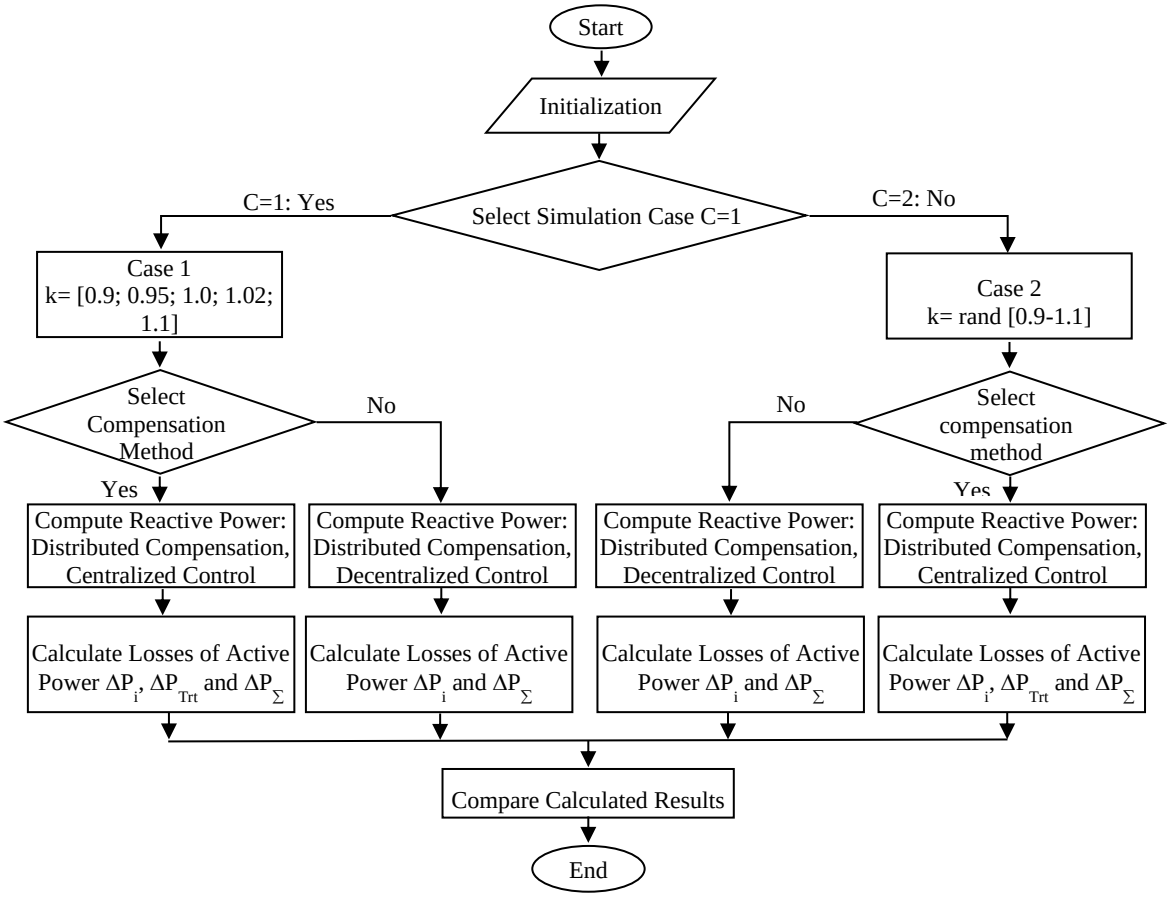

Fig. 3 The flow chart to implement the proposed compensation method in the MATLAB environment

3. Simulations and Practical Applications

Simulation and experimentation are two inseparable aspects of validating the feasibility of a newly proposed control algorithm. The current part focuses on representing the numerical simulations and experimental application of the reactive power compensation method proposed in the previous section.

The flowchart detailing the simulation steps performed in the MATLAB environment is provided in Figure 3, while Figure 2 illustrates the power system under study. The load comprises three large induction motors, with reference parameters outlined in the Appendix. It is pertinent to note that three cases will be simulated: absence of compensation devices, utilization of distributed compensation devices, and employment of distributed compensation devices with centralized control incorporating the proposed Lagrange algorithm. Furthermore, it is assumed that the grid voltage ranges from 90 to 110% of U_{dm}.

The simulation results are comprehensively presented in Table 1 and Figures 4(a) and (b). Figure 4(a) depicts the declining trend of total active power losses as the voltage increases, wherein the total loss curves decrease across all three simulation cases. Notably, the centralized control Distributed Compensation (D-C) method (green solid line) exhibits the lowest values, underscoring the superior performance of the proposed reactive power compensation algorithm.

The distributed control distributed compensation solution (D-D) method (red dashed line) also yields commendable results compared to the uncompensated case, albeit with slightly inferior control quality relative to the centralized control scenario. Revisiting Table 1, it becomes apparent that the reactive power compensation performance of the proposed algorithm achieves the most significant results when juxtaposed with the uncompensated case, registering at 102% (corresponding to a relative active power loss reduction of 34.2%). In comparison to the distributed control distributed compensation case, the optimal outcome is attained at 105% U_{dm}, yielding a relative total active power loss reduction of 11.97%.

Figure 4(b) depicts a more realistic simulation scenario with random voltage fluctuations between 90 and 110%U_{dm}. The simulation results obtained further corroborate the superior performance of the proposed centralized control algorithm for distributed compensation devices. Figures 5 and 6 present the experimental results obtained on actual loads, namely large-capacity functional buildings in Hanoi, the capital of Vietnam. The voltage quality is observed to be satisfactory (the voltage waveforms are nearly horizontal), while the power factor is high (approximately 1). These findings validate the practical applicability of the proposed solution.

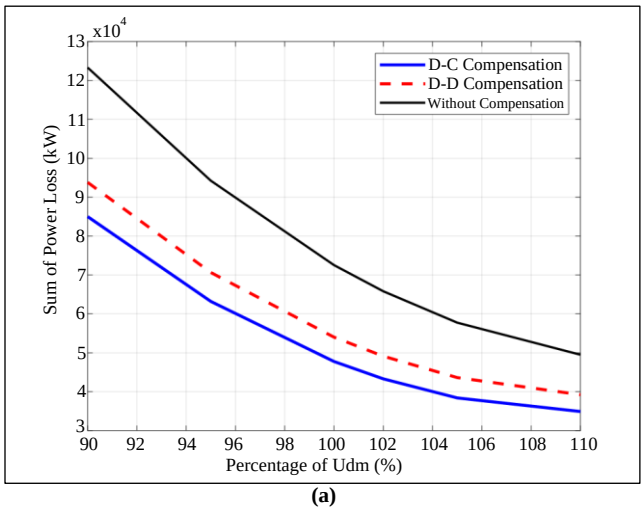

(a)

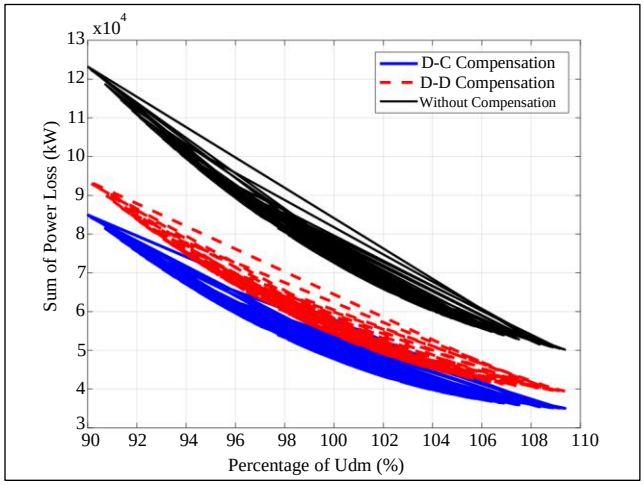

(b)

Fig. 4 Simulation results for the power losses in case of changing voltage between 90% to 110%U_{dm} (a) Step change, and (b) Random change.

Table 1. Computed results obtained for three simulation scenarios

ΔP_{Σ} (kW)	**90%U_{dm}**	**95%U_{dm}**	**100%U_{dm}**	**102%U_{dm}**	**105%U_{dm}**	**110%U_{dm}**
D-C (Decentralized - Centralized)	85005.6	63203.1	47763.2	43303.8	38405.4	34907.8
D-D (Decentralized – Decentralized)	93803.5	70636.0	54015.2	49127.2	43627.3	39225.4
Without compensation	123311.3	94228.0	72534.0	65814.1	57749.9	49503.2
($\Delta P_{\Sigma\ No}$ - $\Delta P_{\Sigma\ D\text{-}C}$) %	31.06%	32.93%	34.15%	**34.20%**	33.50%	29.48%
($\Delta P_{\Sigma\ D\text{-}D}$ - $\Delta P_{\Sigma\ D\text{-}C}$) %	9.38%	10.52%	11.57%	11.85%	**11.97%**	11.01%

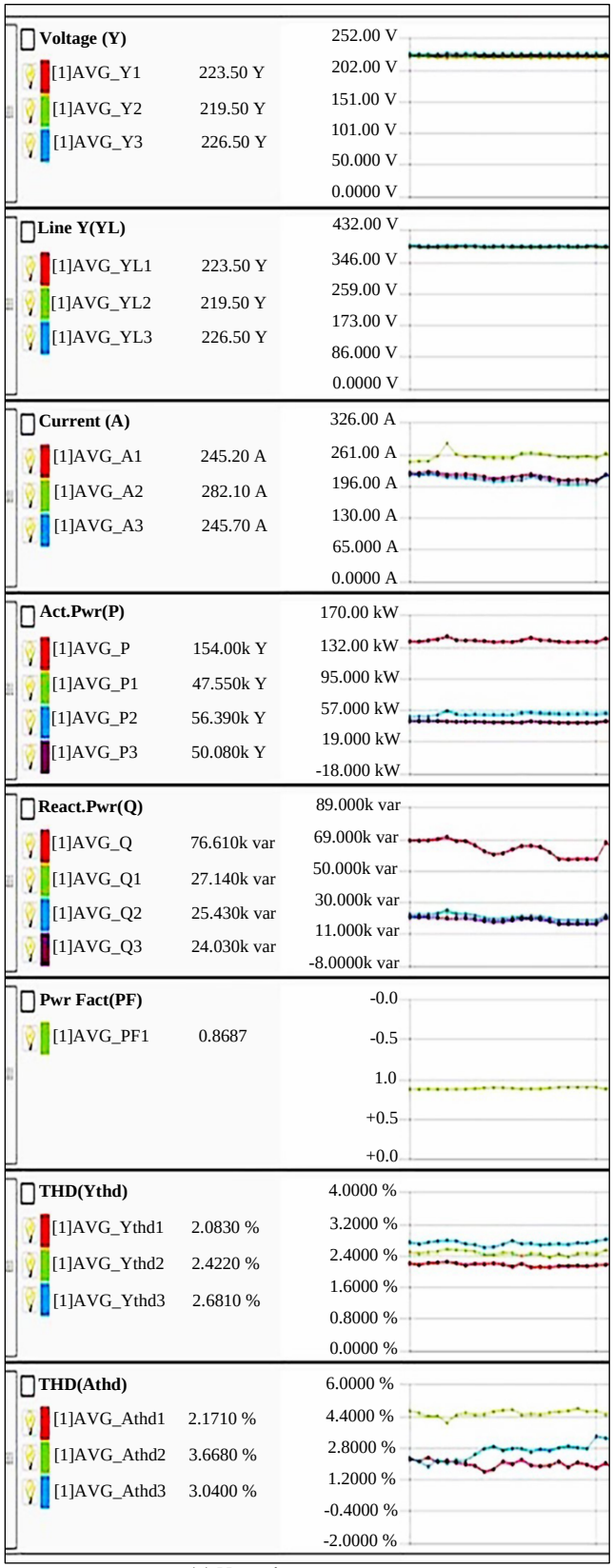

(a) Not using compensators

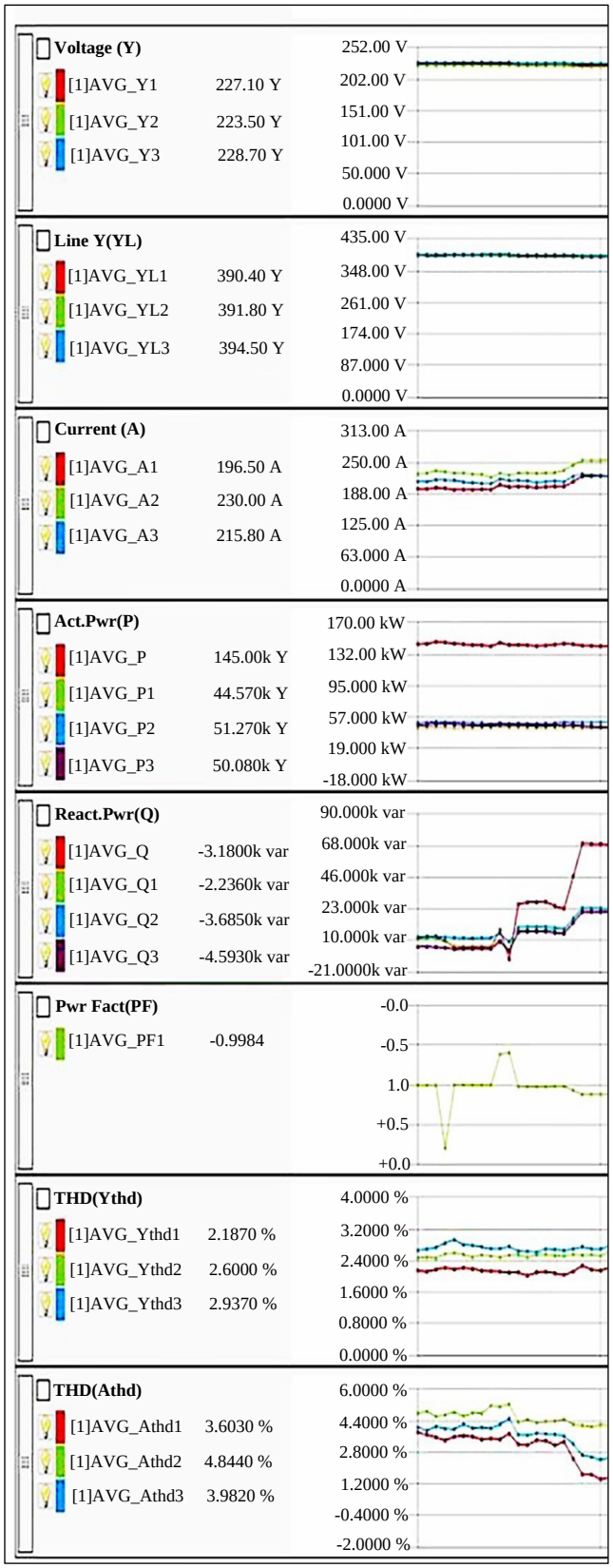

(b) Using the compensators proposed in this study

Fig. 5 Practical applications (a) No compensation, and (b) Compensated with the proposed method.

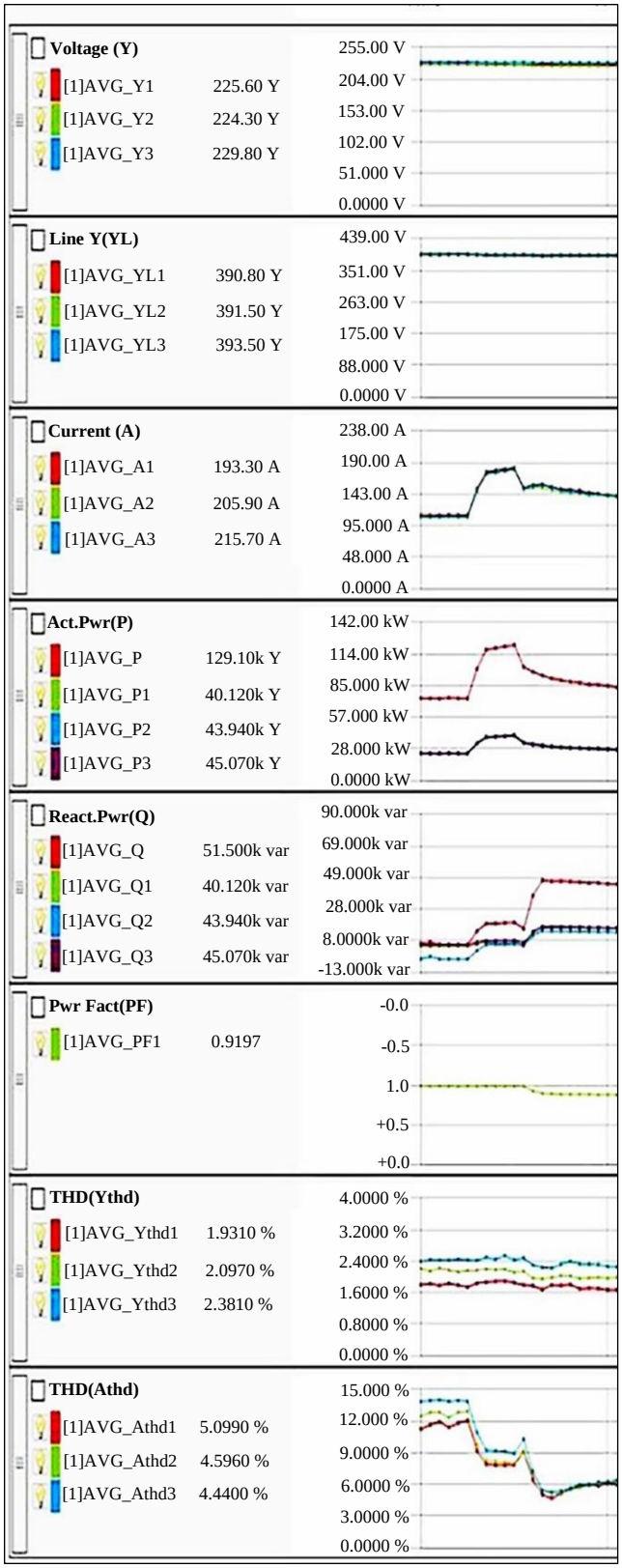

(a) Not using compensators

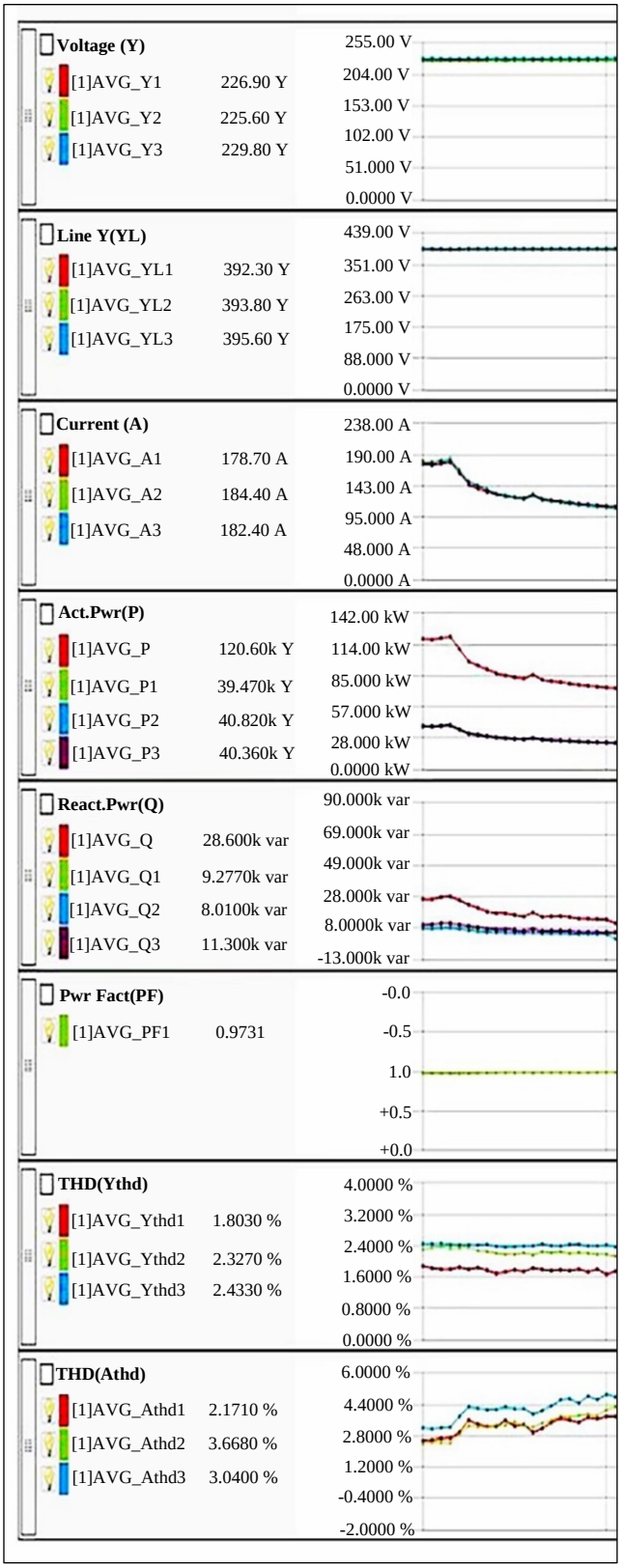

(b) Using the compensators proposed in this study

Fig. 6 Practical results (continued)

4. Conclusion

This study concentrated on analyzing reactive power compensation methods and subsequently selected a simple yet effective strategy based on Lagrange theory. This concept was then integrated with a decentralized compensation scheme and a centralized control strategy to establish a practical methodology for regulating power system voltage, thereby enhancing grid quality. Both simulated scenarios and real-world applications in a relevant test case corroborated the efficacy of the proposed control methodology. Compared to scenarios employing only decentralized compensation or no compensation at all, the proposed scheme achieved demonstrably superior control performance. Future research directions will focus on incorporating novel optimization mechanisms within the proposed control strategy to facilitate its commercialization and widespread application.

References

[1] Omkar Pawar, P. Marshall Arockia Dass, and A. Peer Fathima, "Power Quality Improvement Using Compensating Type Custom Power Devices: A Review," *National Conference on Science, Engineering and Technology*, vol. 4, no. 6, pp. 155-158, 2016. [Google Scholar] [Publisher Link]

[2] Alireza Askarzadeh, "Capacitor Placement in Distribution Systems for Power Loss Reduction and Voltage Improvement: A New Methodology," *IET Generation, Transmission & Distribution*, vol. 10, no. 14, pp. 3631-3638, 2016. [CrossRef] [Google Scholar] [Publisher Link]

[3] S.S. Kanojia, and Suketu Rajyaguru, "Reactive Power Compensation for LV Distribution Network," *International Journal of Innovative Technology and Exploring Engineering*, vol. 8, no. 6, pp. 1734-1741, 2019. [Google Scholar] [Publisher Link]

[4] Xuesong Zhou et al., "A Review of Reactive Power Compensation Devices," *2018 IEEE International Conference on Mechatronics and Automation (ICMA)*, Changchun, China, pp. 2020-2024, 2018. [CrossRef] [Google Scholar] [Publisher Link]

[5] Fedor Nepsha et al., "Application of FACTS Devices in Power Supply Systems of Coal Mines," *E3S Web of Conferences*, vol. 174, pp. 1-8, 2020. [CrossRef] [Google Scholar] [Publisher Link]

[6] Narendra Balkishan Soni, and Avnee Gaur, "A Literature Review on Voltage Regulation Techniques in Power System," *International Journal of Scientific and Research Publications*, vol. 8, no. 5, pp. 270-274, 2018. [CrossRef] [Google Scholar] [Publisher Link]

[7] Aushiq Ali Memon, "*Analyses of Reactive Power Compensation Strategies in Medium and Low Voltage Electrical Network Systems in the Wake of Renewable Energy Infeed*," M.Sc Thesis, Power Engineering, University of Vaasa, 2013. [Google Scholar]

[8] Venu Yarlagadda, K.R.M. Rao, and B.V. Sankar Ram, "Hardware Circuit Implementation of Automatic Control of Static Var Compensator (SVC) Using Micro Controller," *International Journal of Instrumentation, Control and Automation*, vol. 1, no. 2, pp. 54-57, 2011. [Google Scholar] [Publisher Link]

[9] Tarek A. Boghdady, and Youssef A. Mohamed, "Reactive Power Compensation Using STATCOM in a PV Grid Connected System with a Modified MPPT Method," *Ain Shams Engineering Journal*, vol. 14, no. 8, 2023. [CrossRef] [Google Scholar] [Publisher Link]

[10] Hung Khanh Nguyen et al., "Decentralized Reactive Power Compensation Using Nash Bargaining Solution," *IEEE Transactions on Smart Grid*, vol. 8, no. 4, pp. 1679-1688, 2017. [CrossRef] [Google Scholar] [Publisher Link]

[11] Mojtaba Kosari, and Seyed Hossein Hosseinian, "Decentralized Reactive Power Sharing and Frequency Restoration in Islanded Microgrid," *IEEE Transactions on Power Systems*, vol. 32, no. 4, pp. 2901-2912, 2017. [CrossRef] [Google Scholar] [Publisher Link]

[12] T. Yuvaraj et al., "Comparative Analysis of Various Compensating Devices in Energy Trading Radial Distribution System for Voltage Regulation and Loss Mitigation Using Blockchain Technology and Bat Algorithm," *Energy Reports*, vol. 7, pp. 8312-8321, 2021. [CrossRef] [Google Scholar] [Publisher Link]

[13] Liang Sun, Xusheng Jian, and Wenqiang Yuan, "The Application and Practice of the Voltage Reactive Power Optimization Automatic Control System (AVC) in the Power Grid of Wuhu Region," *International Journal of Online and Biomedical Engineering*, vol. 12, no. 2, pp. 10-15, 2016. [CrossRef] [Google Scholar] [Publisher Link]

[14] Shunjiang Lin et al., "Robust Optimal Allocation of Decentralized Reactive Power Compensation in Three-Phase Four-Wire Low-Voltage Distribution Networks Considering the Uncertainty of Photovoltaic Generation," *Energies*, vol. 12, no. 13, pp. 1-20, 2019. [CrossRef] [Google Scholar] [Publisher Link]

[15] Saverio Bolognani, and Sandro Zampieri, "A Distributed Control Strategy for Reactive Power Compensation in Smart Microgrids," *IEEE Transactions on Automatic Control*, vol. 58, no. 11, pp. 2818-2833, 2013. [CrossRef] [Google Scholar] [Publisher Link]

[16] Dimitri P. Bertsekas, *Constrained Optimization and Lagrange Multiplier Methods*, 1st ed., Athena Scientific, 1996. [Google Scholar] [Publisher Link]

Appendix

Table 2. Parameters of motors and cables

Induction Motor i and Cable i	1st Motor	2nd Motor	3rd Motor	Unit
R_i	0.053	0.088	0.070	Ω
X_i	0.009	0.015	0.012	Ω
P_i	160	220	185	kW
Q_i	99.16	136.34	114.65	kVAr
$\cos\varphi_i$	0.85	0.85	0.85	n/a
Δp_{bi}	$0.5*10^{-3}$	$0.5*10^{-3}$	$0.5*10^{-3}$	kW/kVAr